J. Fluid Mech. (1977), *vol.* 81, *part* 2, *pp.* 317-333
Printed in Great Britain

A chemical reaction in a turbulent jet

By JOHN R. SHEA
Department of Mechanics and Engineering Science, Air Force Institute of Technology,
Wright-Patterson AFB, Ohio 45433

(Received 14 July 1976 and in revised form 20 December 1976)

This experimental investigation determines the effect of the various parameters of a subsonic axisymmetric jet upon a fast chemical reaction between ozone contained dilutely in the primary jet and diluted nitric oxide being entrained from the ambient fluid. Radial profiles of ozone densities are determined from absorption measurements of a thin beam of ultraviolet light which is probed across the jet. Data have been obtained for five jet Reynolds numbers between 4000 and 32 000 to reflect variations in both gas density and nozzle velocity; the data confirm Reynolds number independence of reactant concentration profiles to within experimental accuracy. When the non-dimensional chemical reaction rate exceeds a determined value, the ozone profiles are observed to be independent of further increases in the reaction speed. The measured ozone concentration profiles are related directly to the molecular-scale mixing in the jet and to mixing intermittency in the mixing zone in particular.

1. Introduction

The subject of chemical reactions in turbulent mixing zones is one of vast technological importance and arises in practical situations ranging from combustion devices to chemical lasers. The system of interest in this study is a second-order chemical reaction limited by a turbulent mixing rate; it is similar in many respects to a turbulent diffusion flame. One of the two chemical reactants is contained in a primary stream of gas while the other resides in a secondary gas. The two fluids meet in a turbulent mixing zone. The chemical reaction of two gases at the molecular level is well understood; however, at present, the rate of the molecular mixing in a turbulent mixing zone is not well understood and is, therefore, the principal interest of this study.

The research reported here is an experimental investigation which employs a fast chemical reaction to study the mixing process in a turbulent axisymmetric jet flowing into a stagnant ambient atmosphere. The primary jet contains a small amount of ozone in an otherwise inert mixture of nitrogen and oxygen as it emerges from a small contoured nozzle. The ambient atmosphere surrounding the jet consists of nitrogen and varying amounts of nitric oxide. Wherever the gases mix on a molecular scale, the ozone and nitric oxide react as follows:

$$O_3 + NO \rightarrow O_2 + NO_2.$$

Since the reaction can occur only to the extent that local molecular-scale mixing permits, the rate of molecular-scale mixing can be determined from measured concentration profiles of the limiting reactant, ozone.

This reaction was selected for several reasons. First, ozone is almost opaque to ultraviolet light (Griggs 1968) and this presents a method for detecting its presence in the mixing zone. Neither nitrogen nor nitric oxide nor nitrogen dioxide absorbs light at the wavelength employed, 2357 Å (Hudson 1971; Melvin & Wulf 1935; Jones & Wulf 1937). Second, because we can detect very low concentrations of ozone with the optical technique employed, we can minimize the heat release from the reaction and can limit the maximum temperature rise in the mixing zone to a few degrees Celsius. We thus have minimal beam distortion from changes in the index of refraction in the mixing zone and can assume constant-density fluid dynamics. Third, as the reaction is fast at room temperature (Herron & Hine 1973; Johnston & Crosby 1951, 1954), we avoid ignition and extinction problems as well as the flame-stabilization problems common to many combustion studies. Other chemical reactions between ozone, oxygen and oxides of nitrogen are too slow to be of interest during the residence time of fluid in the mixing zone of the jets studied.

This approach to mixing presents an alternative to the use of a density probe, from which the measurement of an instantaneous point quantity is always limited by probe interference with the flow and the space–time volume of the response. In this experiment time-averaged measurements are made of the concentration of ozone, which is a reactant existing locally, as a function of the reactant concentrations in the unmixed gases and of the local proportions of molecular-scale mixing. The unmixed reactant concentrations are always known, and in the limit of fast chemical kinetics we can relate the measured time-average ozone concentration directly to the statistical properties of the local, instantaneous mixing proportions of the turbulent jet. The spatial resolution of the measurement only needs to be sufficient to discern detail in the mean profiles. The only physical interaction between the jet and the measurement technique is through a very faint beam of ultraviolet light.

The geometry of the experiment is designed for maximum simplicity. The reacting jet is enclosed in a tank, which initially holds the stagnant NO, N_2 mixture. The nozzle for the ozone jet enters vertically from the top and extends an adjustable distance into the tank. The optical system is fixed to the side of the tank and sweeps across the jet in a horizontal plane during each run. The light source is the 2357 Å band of a low pressure mercury lamp, and a photomultiplier tube measures light intensities while an automatic digital data acquisition system records the measurements. The measured absorption profiles can be readily converted into radial ozone concentration distributions.

The experimental programme is directed towards answering four basic questions about the turbulent, chemically reacting jet.

(i) How is the overall reaction rate related to the basic parameters of the jet?

(ii) What is the effect of jet Reynolds number on the mixing process?

(iii) When is the chemical reaction fast enough to produce a mixing-limited jet profile?

(iv) What are the implications of the data for the problem of molecular mixing in the jet?

2. The experimental programme

The experimental programme consists primarily of measuring profiles of ozone density as a function of radial distance from the jet centre-line at four axial distances from the nozzle: 1, 2, 3 and 5 diameters downstream. We measure both non-reacting profiles for ozone spreading into a tank filled with pure nitrogen and reacting profiles of ozone spreading into a tank containing nitrogen mixed with various amounts of the reactant nitric oxide. The ozone profiles of non-reacting jets determine time-averaged entrainment rates and the mean fraction of gas originating in the primary jet at points throughout the mixing zone. Measurements on reacting jets yield the mean molar density of gas originating in the primary jet which remains locally unmixed with the ambient fluid. Most of the experimental data consist of reacting and non-reacting ozone profiles for five different Reynolds numbers, based on nozzle diameter and ranging from 4000 to 32 000, and for two tank pressures, 1·34 and 4·06 atm.

The basic measurement in the experiment is quite simple in concept. A signal proportional to the intensity of a collimated beam of the filtered 2537 Å line from a mercury lamp can be measured with a photomultiplier tube. The ratio of two measurements, one with and the other without ozone present, determines the attenuation of the beam, and the logarithm of this intensity ratio is proportional to the number of molecules of ozone in the volume illuminated by the beam:

$$\ln I_0/I = \int \alpha n_{\mathrm{O}_3}\, dy, \qquad (2.1)$$

where I and I_0 are the measured light intensities, in volts, with and without ozone present, α is the absorption coefficient for ozone at 2537 Å[$1{\cdot}14 \times 10^{-16}$ cm^2/molecule; Griggs 1968) and y is the ordinate along the optical path. In this work the variable N will refer to the initial concentration (molecules/cm^3) of the subscripted chemical species in unmixed fluid. The variable n will represent the concentration of the subscripted species in the mixing zone of the jet. As the temperature is always within a few degrees of 295 °K in the experiment, N and n are proportional to both mass density and partial pressure.

Despite the simplicity of the basic measurement, the experiment entails certain practical difficulties. Ozone, oxygen and some oxides of nitrogen can explode if exposed to grease or combustible materials. Ozone decomposes on contact with container walls unless extreme care is taken in both design and maintenance. Most of the gases are not only poisonous but also corrosive to many common materials of construction and to most sensitive laboratory equipment.

The experimental parameters are

$$N_{\mathrm{O}_3}, N_{\mathrm{NO}}, N_{\mathrm{Tank}}, u_0; \quad k, d, D, \Delta H_f, C_P,$$

where:

N_{O_3} = ozone concentration (molecules/cm^3) in unmixed primary jet,
N_{NO} = nitric oxide concentration (molecules/cm^3) in unmixed ambient fluid,
N_{Tank} = total molecular density in experimental tank (molecules/cm^3),
u_0 = nozzle velocity (cm/s),
k = chemical kinetic rate coefficient for ozone and nitric oxide
= $1{\cdot}12 \times 10^{10}$ cm^3/mole s at 23 °C,

d = nozzle diameter = 0·508 cm,

D = molecular diffusivity of jet gas (cm^2/s), which is here equal to the kinematic viscosity μ/ρ for nitrogen as the Schmidt number is approximately 1·0 for all chemical species,

ΔH_f = heat of reaction for $O_3+NO \rightarrow O_2+NO_2$, which is exothermic at 47·7 kcal/mole (Herron & Hine 1973),

C_P = heat capacity of the gas (nitrogen) = 6·97 cal/mole °K,

T = absolute temperature = 295 °K for all runs.

The first four parameters listed are varied in the experimental programme. They can be organized into four non-dimensional groups, each with a physical meaning:

$u_0 d/D$, the Reynolds number;
$N_{O_3}\Delta H_f/N_{\text{Tank}}C_P T$, the dilution number;
$kN_{NO}\,d/u$, the reaction-speed number;
N_{NO}/N_{O_3}, the concentration ratio.

The Reynolds number

Of the four non-dimensional numbers listed above, the Reynolds number Re appears to be the most likely to affect the molecular mixing rate. But the Reynolds number should affect the overall mixing rate only if diffusion on the smallest length scales in the turbulence limits the mixing process. Five different Reynolds numbers are investigated in this study: 12 500, 5000, 15 000, 4000 and 32 000. The first two are run at an overall tank pressure of 1·34 atm and the last three at a tank pressure of 4·06 atm.

Two characteristic time scales can be associated with each case. The first is a convective time scale τ_c associated with the breakdown of large eddies:

$$\tau_c = d/u_0.$$

The second is a diffusive time scale τ_D associated with molecular diffusion on the Kolmogorov length scale:

$$\tau_D = d/u_0 Re^{-\frac{1}{2}}.$$

The values of τ_c in this experiment range from $1{\cdot}8\times10^{-3}$ to $4{\cdot}6\times10^{-4}$ s; the values of τ_D range from $1{\cdot}2\times10^{-6}$ to $2{\cdot}7\times10^{-5}$ s. One would therefore expect the breakdown of the large-scale eddies to be the rate-limiting mixing process. The Reynolds number independence observed in the present measured concentration profiles, as well as in the studies of diffusion flames by Hawthorne, Weddell & Hottel (1949), Wohl, Gazley & Kapp (1949), Hottel (1952) and Yagi & Saji (1952), supports this view.

The dilution number

The addition of chemically reacting species to the jet and ambient fluid can have two effects on the jet properties. First, the addition of chemical species can change the density of the carrier fluid; this effect is extremely small for the mixtures used in this experiment. Though additives may not affect the jet density, dilute chemical species can have a marked influence on the flow through a second effect: the heat release from chemical reactions. In common examples of combustion this effect dominates the reaction zone. The heat of reaction released in the jet is

$$\text{heat in} < N_{O_3}\Delta H_f \quad (\text{cal/cm}^3). \tag{2.2}$$

Here the heat per unit volume is less than the expression in (2.2) because the ozone-containing primary jet must be mixed with some nitric-oxide-containing ambient fluid before the energy is released. Since the heat capacity of the gas is

$$N_{\mathrm{Tank}} C_P \quad (\mathrm{cal/cm^3\,^\circ C}),$$

we can calculate the maximum change in temperature or density ρ due to the heat of reaction as follows:

$$\frac{\Delta T}{T} = -\frac{\Delta\rho}{\rho} < \frac{N_{\mathrm{O_3}} \Delta H_f}{N_{\mathrm{Tank}} C_P T} = 0{\cdot}02\text{–}0{\cdot}05. \tag{2.3}$$

For the experiments this number was kept low, to a maximum temperature rise of about 16 °C, by limiting the partial pressure of ozone in the primary jet to 0·003 atm in most runs. At ozone partial pressures below 0·01 atm no heat-release effects have been noted.† In this experiment the dilution number is not an important parameter group.

The reaction-speed number

Chemical non-equilibrium in the mixing zone depends on a non-dimensional reaction rate: the reaction-speed number. The papers by Herron & Hine (1973) and Johnston & Crosby (1951, 1954) on the chemical kinetics of ozone and oxides indicate that mixed ozone and nitric oxide undergo the reaction

$$\mathrm{O_3 + NO \rightarrow O_2 + NO_2} \tag{2.4}$$

to produce a decay of the ozone

$$d(\mathrm{O_3})/dt = -k(\mathrm{NO})\,(\mathrm{O_3}), \tag{2.5}$$

the values in parentheses being concentrations of the chemical species indicated. The characteristic time for the chemical reaction is then

$$\tau_{\mathrm{chem}} = 1/kN_{\mathrm{NO}}, \tag{2.6}$$

which varies from $1{\cdot}6 \times 10^{-4}$ to $1{\cdot}6 \times 10^{-5}$ s in this experiment. The reaction-speed number is the ratio of two characteristic times of the turbulent reacting jet:

$$kN_{\mathrm{NO}}\, d/u = \tau_c/\tau_{\mathrm{chem}}. \tag{2.7}$$

We can briefly consider two limits of the reaction-speed number. When this number is small, the rate of the chemical reaction is the slowest step of the mixing and reaction process. The jet carries fully mixed chemical reactants which have not had time to react; this is the limit of frozen chemistry. When the reaction-speed number is large, however, we approach the limit of equilibrium chemistry. The overall reaction rate is again controlled by the rate of the breakdown of the largest eddies because the reaction time is the shorter of the two processes. In this case the jet is mixing limited.

---

† An effect of heat addition was noted in preliminary experiments in which the ozone partial pressure exceeded 0·015 atm. Bright spots of intensity 5 % higher than the blank measurement appeared at either edge of the profile at axial positions less than two diameters from the nozzle. The heated gas in the jet was acting as a lens and focusing light at the edge of the jet.

The concentration ratio

The concentration ratio is an important parameter in the turbulent reacting jet. When profiles are Reynolds number independent, mixing limited and not affected by the dilution number, the concentration ratio is the only parameter remaining to characterize the reaction zone. The concentration ratio can be directly related to the turbulent-flow flame length (Hawthorne *et al.* 1949; Wohl *et al.* 1949; Hottel 1952; Yagi & Saji 1952) by first computing a flame length for a laminar jet and then substituting a constant eddy diffusivity for the molecular diffusivity.

The extent of the reaction zone of a turbulent jet can also be related to the concentration ratio by considering the probability of observing a mixture with a mixing fraction above a critical value at a given point in the flow. For a given reactant concentration ratio we can define a critical mixing fraction η_0 (η = number of moles of primary gas/total number of moles present in sample) at which the chemical reactants combine in exact stoichiometric proportions. In the ozone/nitric-oxide system of this experiment, we find ozone in mixtures with $\eta > \eta_0$ and nitric oxide in mixtures with $\eta < \eta_0$. Since a flame or chemical reaction will persist wherever some reactant from the primary jet remains, the edge of the reaction zone occurs where the probability of observing mixtures with $\eta > \eta_0$ drops to zero.

In this experiment we use low ozone concentrations in the primary jet and high concentrations of nitric oxide in the ambient fluid; typical values of η_0 are 0·90–0·98, corresponding to concentration ratios of 10–50. In this limit ozone is consumed in almost all the gas actually within the turbulent mixing volume of the jet. Only bits of potential fluid from the core of the jet contain unreacted ozone, and these extend to a reaction length of only slightly over 5 diameters. Also in this limit, as the excess concentration of nitric oxide consumes ozone out to the edge of the turbulent/non-turbulent interface, the profiles become independent of concentration ratio as well as the other parameters.

3. The experimental apparatus

Elements of the experimental apparatus fall into one of four categories. The first is a contoured nozzle, which produces the axisymmetric jet. The nozzle is fed by a gas delivery system, which supplies ozone, nitrogen and nitric oxide to the nozzle and experimental tank. The third equipment system includes the experimental tank, which contains the turbulent jet. Finally, an optical system measures all ozone concentrations and is connected to a digital data acquisition system which automatically records the data. Each of the four categories will be described in turn.

The nozzle used in this experiment was carefully designed to produce uniform and axially symmetric flow. The interior of the nozzle contains several layers of 218 mesh screens in a 2·5 cm diameter settling chamber. The nozzle contour consists of a contraction section with a radius of curvature of 1·0 cm followed by a 0·25 cm straight section. The exit diameter measures 0·508 cm ± 0·002 cm, producing a 25:1 area contraction from the settling chamber to the exit. This is sufficient to produce smooth and uniform flow across most of the nozzle exit; a hot wire placed in the opening of the nozzle in a preliminary test measured turbulence levels of less than 0·3 %.

A potential core in the jet extends to almost 3 diameters from the nozzle, a somewhat

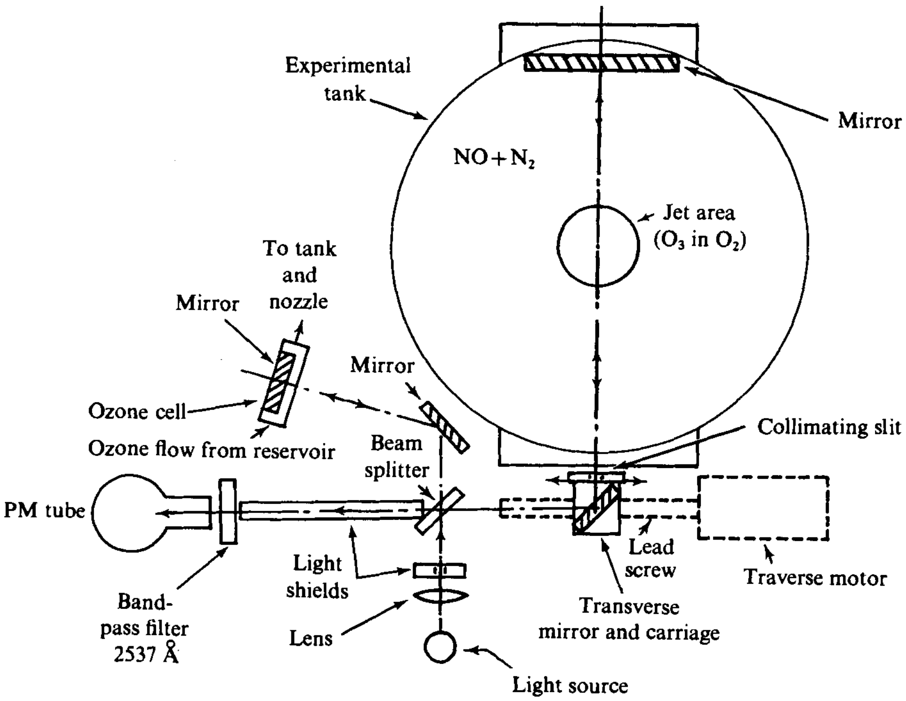

FIGURE 1. Optical system for experiment on chemically reacting jet.

shorter core than those observed by other investigators (Bradshaw, Ferriss & Johnson 1964; Davies, Fisher & Barratt 1963; Kuethe 1935), who typically report 4–6 diameters of potential core. Thick boundary layers, estimated to extend across 10 % of the nozzle-exit diameter, appear to account for the discrepancy. The presence of the boundary layers in the nozzle also produces a 5 % discrepancy between the mass-averaged velocity, which is measured, and the actual velocity of the jet potential core. A velocity correction was not made for the data presented in this work, however, and the stated nozzle velocities are always the measured mass-averaged velocities unless otherwise indicated.

The gas delivery system consists of equipment which supplies the four gases, nitrogen, nitric oxide, oxygen and ozone, to the experiment. Caltech and Linde high-purity dry-grade nitrogen comprises the bulk carrier gas of the experiment, and Matheson and Linde technical-grade (98·5 % pure) nitric oxide from gas cylinders is used. An ozonier converts bottled oxygen to ozone, which is then stored briefly in a special ozone cylinder. The ozone is next diluted with nitrogen and pressurized to the desired delivery pressure in preparation for the experimental run. An exhaust system empties the experimental tank after each run and partially absorbs noxious gases used in the experiment.

The fluid dynamics of primary interest to this investigation take place in the experimental tank, a 238 l vessel almost 2 m high and 0·5 m in diameter. Starting transients, on the one hand, and the recirculation of gas in the tank from the nozzle to the tank bottom and finally back into the jet itself, on the other, limit the running time of experiments. Steady run times vary from 3 to 7 s in the cases considered.

The optical system is designed to make the two primary ozone concentration measurements and represents the heart of the entire experimental apparatus. The schematic diagram of the optical system (figure 1) shows four arms of the system spreading out from a beam splitter. One arm contains a mercury lamp and another holds a photomultiplier tube to monitor light intensity. One of the other two arms leads to the ozone cell, which monitors nozzle-inlet ozone concentration, and the other effects the measurement of the ozone concentration profile in the jet.

The light source for the experiment is a low pressure d.c. mercury lamp, and the opening in the shield over the lamp is a pin-hole 0·5 mm in diameter. The lamp emits high intensity light, drifts reasonably little, has a reasonably low noise level, and radiates most of its energy at 2537 Å, which is the ultraviolet wavelength used for all absorption measurements.

The ozone cell is located in the optical-system arm opposite the mercury lamp. It contains a quartz viewing window and an internal quartz-coated front-surface mirror. A splitter plate 1·27 ($\pm$ 0·013) mm thick separates the window from the mirror, and spring loading the mirror against the window prevents any internal slippage.

The arm of the optical system which passes through the experimental tank is by far the most difficult part of the experiment to design. As indicated in figure 1, the light travels from the beam splitter to a 45° front-surface mirror on the traversing carriage, through the limiting aperture attached to the tank side of the carriage, through the tank to an internally mounted front-surface mirror then back the way it came. Major problems come from the need for temporal and spatial resolution. The beam must sweep the entire width of the jet in the 3–7 s of steady-state operation of the jet. The beam has a cross-section 0·25 mm wide and 0·50 mm high, and the tank width of 0·5 m requires that the beam remains collimated over a 1 m path length while the carriage is in motion. The signal level produced by a lens and a mercury lamp is very low, particularly in this arm of the optical system. The light intensity is typically of the order of 20000 photons/ms and is too low to affect the overall chemistry of the jet. No ultraviolet lasers were available for the experiment.

Two measurements of intensity *vs.* position are required for each run. One, of I_0 *vs.* x, records the beam intensity in the vicinity of the jet with no ozone present and is made just before the measurement of I *vs.* x during steady-state jet operation. The profiles are quite reproducible, and the correspondence of I_0 to I at either edge of the jet provides verification of the system's stability during each run.

The two optical-system signals, the beam's position and intensity, are recorded on a digital recording system, designed by Prof. Donald Coles of Caltech in 1971 and consisting of a mobile analog-to-digital converter interfaced to a synchronous digital tape recorder. The a/d converter converts $\pm$ 10 V signals to a 12 bit binary code with a resolution of approximately $\pm$ 0·005 mV.

4. The reduction of the absorption profiles

Having measured a light-absorption profile $H(x)$ associated with a set of experimental parameters, we next approach the problem of reducing the data to ozone concentration distributions in each case. The data consist of the logarithm of the ratio of two experimental measurements, $I_0(x)$ and $I(x)$, and are related to the time-averaged jet ozone concentration by

$$H(x) = \frac{1}{2\alpha}\ln(I_0/I) = \int_{-\infty}^{\infty} n_{O_3}(r)\,dy, \tag{4.1}$$

where $r^2 = x^2+y^2$ and y is along the optical axis. Solving the integral equation is related to the classical problem of Abel inversion.

Errors in each intensity measurement of 2–3 % can produce an uncertainty of nearly 10 % in the logarithmic intensity ratio. Thus the sensitivity of the results of the mathematical procedures to experimental noise will be a primary concern.

Two features of the ozone concentration profile are evident from consideration of the normalized intensity profiles: the ozone spreading rate and the average of the ozone concentration across a jet cross-section. In view of the sensitivity to experimental noise inherent in further breakdown of the data to profiles of ozone concentration against radial position, we shall consider these results before discussing the results of the Abel inversion procedure.

The ozone spreading rate

The spreading rate of the ozone-bearing part of the jet can be inferred from the simple observation of the widths of absorption profiles at a number of axial stations downstream of the nozzle. The jet ozone concentration radius is defined as the distance from the jet centre-line to the point where $\ln(I_0/I)$ falls to 0·05, a value just above the typical experimental random noise level. In processing data from profiles with very low ozone levels, care was taken to distinguish between the crossing of a mean intensity level and any premature crossing due to noise spikes in the data. In a non-reacting jet, the similarity between mass and momentum transport ensures that the jet ozone radius is a measure of the cross-sectional area of the turbulent jet itself. In the reacting jet, the ozone radius falls inside the non-reacting ozone radius because of depletion of ozone by chemical reaction at the outer edge of the jet. In short, the ozone concentration radius is a measurement of the extent of the ozone-bearing part of the jet.

The axisymmetric jet of this experiment differs from ostensibly similar jets examined in other studies in that the mixing zone spreads somewhat more rapidly. The jet radius doubles to 1 diameter by axial distances of 2–2·5 diameters downstream. Pitot surveys and concentration profiles both indicate that the potential core of unmixed gas at the centre-line of the jet ends at approximately that same axial position (3 diameters). The shear layer in the initial mixing zone thus spreads symmetrically, inwards and outwards, but the potential core is shorter than the 4 diameters generally observed in other studies (Bradshaw *et al.* 1964; Davies *et al.* 1963; Kuethe 1935). Unavoidable thick boundary layers are largely responsible for the discrepancy.

Absorption measurements in cases of a great excess of NO in the ambient fluid show a non-spreading ozone region. The data indicate that the ozone molecules at the outer edge of the highly reacting jet are mixed with and consumed by the nitric oxide in the ambient tank fluid. Within the first diameter, the ozone concentration edge spreads to a total width of 1·5 diameters (± 0·26) and holds approximately constant out to 5 diameters, at which point the overall ozone levels are so low that the profile becomes difficult to measure.

The average of the ozone concentration across the jet cross-section

The second jet characteristic available from the simple measurement of the light intensity ratio is the ozone concentration integral. We directly measure the intensities at points x along the beam's direction of traverse and relate these measurements to the ozone concentration through (4.1). Integrating the measurements with respect to x, we find that the ozone concentration integral (over the jet cross-section) is

$$\int H(x)\,dx = \iint_{-\infty}^{\infty} n_{O_3}(r)\,dy\,dx = \iint n_{O_3}\,dA. \tag{4.2}$$

The cross-sectional average of the ozone density is the physical quantity best associated with the ozone concentration integral. Having calculated the ozone concentration integral and knowing the jet cross-sectional area from its relation to the ozone concentration radius R in the non-reacting jet, we find the average of the ozone concentration over a cross-section by taking the quotient of the two:

$$\overline{n_{O_3}(z)} = \frac{1}{\pi R^2}\iint n_{O_3}\,dA. \tag{4.3}$$

The ratio of reacting (subscript R) to non-reacting (subscript N) average ozone concentration is the corresponding indicator of the effect of reaction on the profile. In that ratio the jet cross-sectional area cancels out and

$$\frac{(\overline{n_{O_3}})_R}{(\overline{n_{O_3}})_N} = \frac{\iint (n_{O_3})_R\,dA}{\iint (n_{C_3})_N\,dA} = \frac{(\int H(x)\,dx)_R}{(\int H(x)\,dx)_N}. \tag{4.4}$$

Conclusions from the integrated ozone profiles

Having selected the ratio of reacting to non-reacting ozone concentration integral (to be referred to as the 'reacting ratio' for brevity) as an appropriate measure of the chemical reaction's effect on the entire profile, we can next consider the variations of the profile with the reaction-speed number, Reynolds number and concentration ratio.

The first project is to derive a value of the reaction-speed number above which we can assume infinitely fast chemistry. With infinitely fast chemistry we can make the important assumption that ozone and nitric oxide cannot coexist at the same location at any instant of time; this will greatly simplify understanding the problem of mixing and chemical reaction. An axial position of three diameters was selected for primary consideration for several reasons. First, profiles show the effects of reaction strongly at this point, the reacting ratio being 0·20–0·40 in most experiments run. Second, other measurements show that the potential core has essentially disappeared by three diameters, leaving the full time-averaged jet cross-section turbulent and characterized by intermittency and mixing interfaces. Finally, enough ozone remains in all cases to produce an adequate signal-to-noise ratio.

Figure 2 shows a plot of the reacting ratio against the reaction-speed number for several measurements at three diameters from the nozzle with concentration ratios of 12·5 (± 2·5). The figure is consistent with a three-dimensional plot (reacting ratio *vs.* reaction-speed number and concentration ratio) of approximately 40 experimental measurements in indicating that at reaction-speed numbers in excess of 8·0 the profiles are independent of the reaction-speed number.

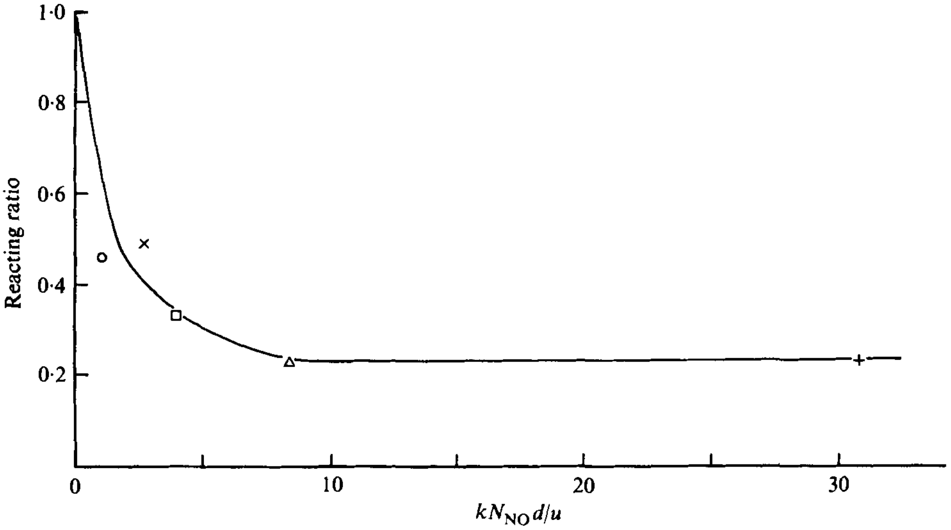

FIGURE 2. Reacting ratio [equation (4.4)] *vs.* reaction-speed number for $z/d = 3$. ○, $Re = 12500$, $P_{Tank} = 1{\cdot}34$ atm; ×, $Re = 5000$, $P_{Tank} = 1{\cdot}34$ atm; △, $Re = 15000$, $P_{Tank} = 4{\cdot}06$ atm; +, $Re = 4000$, $P_{Tank} = 4{\cdot}06$ atm; □, $Re = 32000$, $P_{Tank} = 4{\cdot}06$ atm.

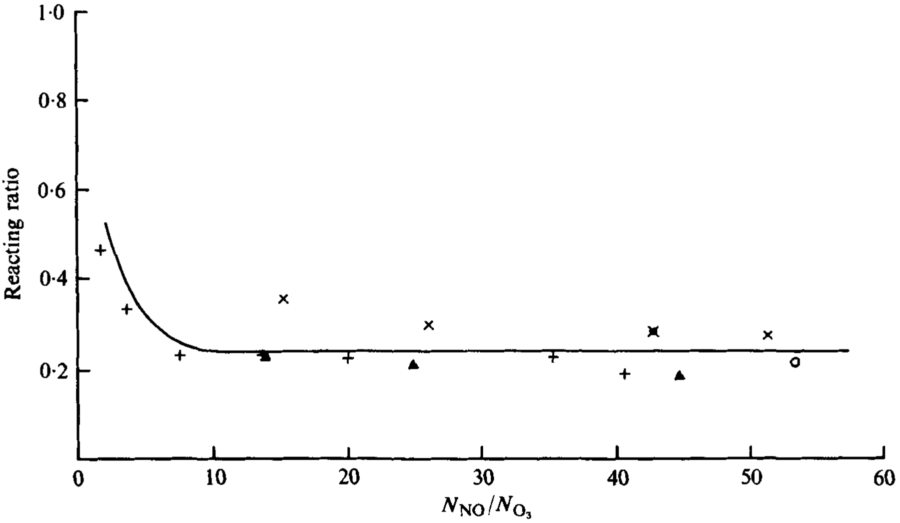

FIGURE 3. Reacting ratio [equation (4.4)] *vs.* concentration ratio for $z/d = 3$. Symbols as in figure 2.

More precise experiments may indicate a threshold of infinitely fast chemistry which varies somethat with position. For instance, distances closer to the origin than three diameters allow less time for cumulative effects of chemical reaction to affect the profile. A constraint of the form

$$kN_{NO}z/u > 24 \tag{4.5}$$

was considered in order to take different axial positions into account, but was not adopted. To a certain extent, experimental noise in the experiment makes the definition

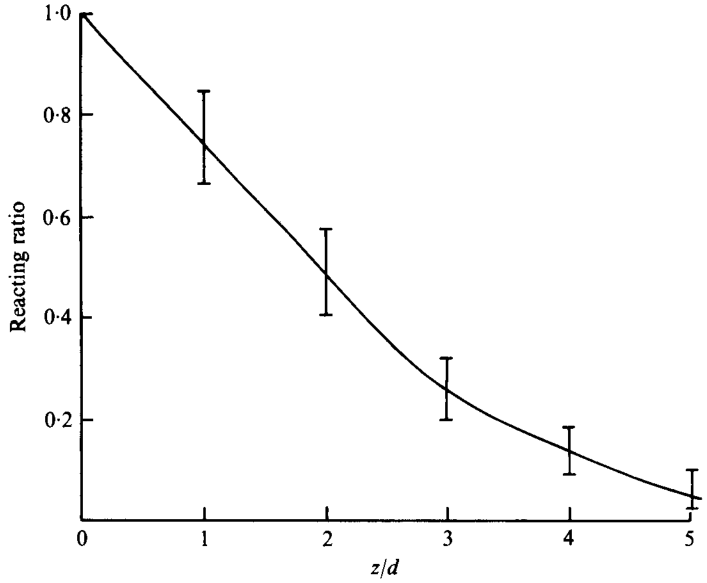

FIGURE 4. Reacting ratio *vs.* axial distance from nozzle exit for all profiles satisfying the criteria (4.6*a*, *b*) for a reacting jet.

arbitrary. It would eliminate from consideration some data at one and two diameters at present included, but the basic trend of the curves shown would change very little. Equation (4.6*a*) appears to be the best definition of a mixing-limited jet for this work.

Figure 3 shows a plot of the reacting ratio against the concentration ratio $N_{\mathrm{NO}}/N_{\mathrm{O_3}}$ at an axial station three diameters from the nozzle for a series of runs under the constraint that the reaction-speed number exceeds 8·0. In examining figure 3, one notices a definite levelling-off of the reacting ratio at values of the concentration ratio greater than ten. This regime,

$$kN_{\mathrm{NO}}\,d/u > 8, \quad N_{\mathrm{NO}}/N_{\mathrm{O_3}} > 10, \qquad (4.6a,b)$$

yields the precise definition of the highly reacting jet mentioned in this work. Consideration of data at one, two and five diameters indicates that these criteria are appropriate there as well.

The presence of a non-zero asymptote at large concentration ratios in figure 3 has an important relationship to the presence of unmixed regions in the flow when we have a mixing-limited jet. If all regions in the mixing zone of a jet were mixed with ambient fluid to some significant extent, then increasing the concentration ratio of a fast chemical reaction should ultimately consume all ozone in the mixing zone. The presence of a non-zero asymptote indicates that some fluid within the jet remains completely unmixed on a molecular level.

Figure 4 shows average reacting ratios for all experiments run under the conditions for a highly reacting jet for each Reynolds number studied. The results are plotted against axial position. The point where the average of the ozone concentration across the jet cross-section becomes zero defines the length of the reaction zone in the limit of a highly reacting jet to be slightly over five diameters. This is much shorter than corresponding flame lengths in studies of turbulent flames (Weddell 1941; Kent & Bilger 1972) as discussed above.

The area of interest *vis-à-vis* finding unmixed gas from the primary jet extends from the nozzle exit out to five diameters down the jet centre-line. Beyond that point observed levels of unreacted ozone are too low to be measured accurately. This is an awkward region of the jet in which to work, particularly as the jet's potential core ends at slightly over two diameters. Data are available in the literature (Kuethe 1935) for a quasi-similarity region extending from the nozzle for a few diameters downstream, where the shear-layer thickness is small compared with the radius of curvature. In this experiment, the mixing-layer thickness is less than the radius of curvature only at the station one diameter from the nozzle. At this station data scatter arises from laminar–turbulent transition causing small shifts in the virtual origin. Jets do not reach a far-field similarity regime until at least ten diameters from the nozzle. Therefore, most of the measurements of this experiment are in a transitional region in which the circumferential shear layer of the initial mixing zone transforms itself into a classical axisymmetric jet at axial distances greater than ten diameters.

The radial ozone profile $n_{O_3}(r, z)$

Although the average ozone concentration is an important indicator of changes in the profile, the average conceals the detailed physics of the mixing process. By taking an average across the entire jet cross-section, we obscure all spatial variations in the time-averaged mixing ratios. Thus the information needed to construct even the most naive eddy-diffusivity model for the mixing process is lost. Further, the average in no way distinguishes molecular unmixedness associated with intermittency in turbulent regions of the jet from unmixed regions in the potential core near the nozzle exit.

We next return to the basic data record of the experiment and consider the inversion of (4.1) to compute the radial ozone concentration distribution $n_{O_3}(r,z)$ for each run. Two approaches were originally used to apply the Abel inversion to the data of this experiment. The first was a direct application of an exact solution to the integral equation. Mathematically, the procedure works well, but the results are highly sensitive to experimental noise. The second approach assumes an appropriate family of density-profile shapes and uses the integral equation (4.1) to evaluate various parameters of the profiles by comparison with the observed data. This was the approach used for the full data analysis.

The second approach to applying the Abel inversion abandons the attempt to calculate the concentration at each point from a single data record. Instead, the following family of allowable ozone profile shapes is assumed:

$$n_{O_3} = \left\{ \begin{matrix} n_1, & r \leqslant c, \\ n_1 \exp\left[-(r-c)^2/a^2\right], & r > c, \end{matrix} \right\} \tag{4.7}$$

where we have three parameters: n_1, a and c. Instead of calculating an entire profile from the data, we look for only the three parameters, which determine an approximate size of the profile. In the process we are guaranteed a physically realistic concentration profile, and errors are distributed over the entire profile instead of concentrated at the centre-line.

The profile parameters each have physical significance. The centre-line density n_1 is always an important profile parameter. In addition, we know that a potential core of unmixed fluid exists near the centre-line for the first few diameters downstream of the

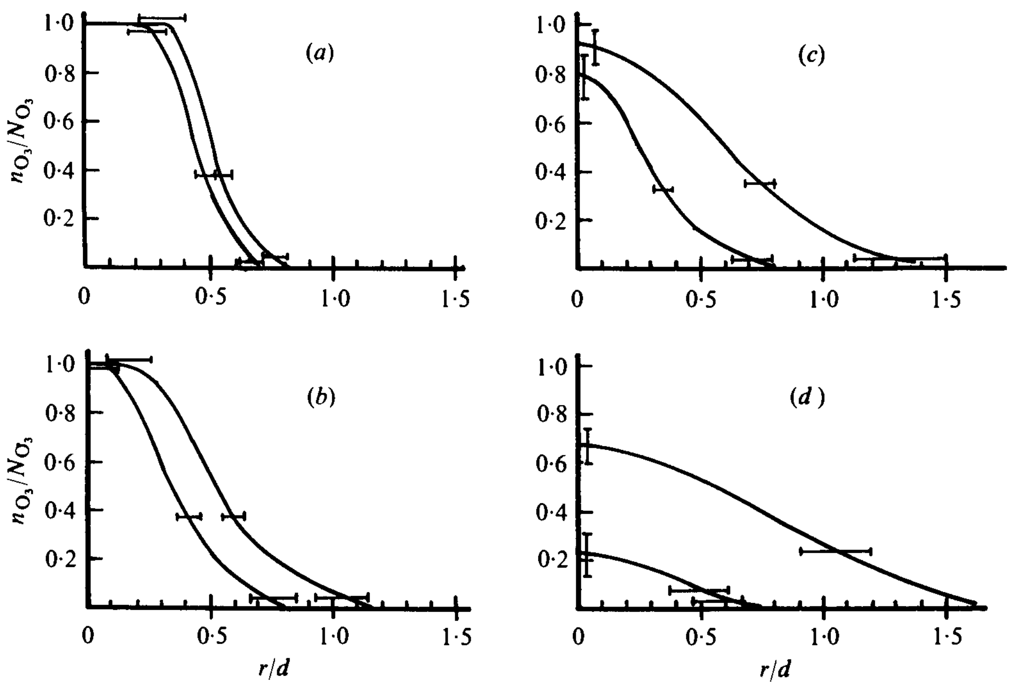

FIGURE 5. Radial ozone concentration profiles drawn from the parameters of (4.7). In each case the outer curve represents a non-reacting jet and the inner the highly reacting jet [equation (4.6)], and data are averaged over all the Reynolds numbers.

nozzle. Being unmixed, this fluid's concentration would be constant out to the core radius c. The parameter a is a characteristic width of the mixing zone of the profile.

If we transform the assumed ozone concentration profile by using the integral equation (4.1) for the observed data, we derive a three-parameter family of intensity profiles:

$$H(x-x_0) = \int_{-\infty}^{\infty} n_{O_3}(r)\,dy = 2n_1 a\, S(c/a, x/a). \qquad (4.8)$$

This formula is quite easy to handle as it may be expressed as a few parameters times a tabulated special function of two variables:

$$S(c/a, x/a) = \left\{ \begin{array}{ll} S_0 + \displaystyle\int_{S_0}^{\infty} \exp\left[-(r-c)^2/a^2\right] d(y/a), & x < c, \\ \displaystyle\int_{0}^{\infty} \exp\left[-(r-c)^2/a^2\right] d(y/a), & x > c, \end{array} \right\} \qquad (4.9)$$

where $S_0 = c^2/a^2 - x^2/a^2$. A standard nonlinear curve-fit procedure selects the three parameters n_1, a and c as well as a fourth, the position x_0 of the centre-line of the jet, to minimize the mean-square variation of the computed profile from the data. The calculation of x_0 is almost completely uncoupled from the other calculations.

The actual conversion of intensity into concentration is exact. The assumptions made only introduce additional information for the calculation. As long as the computed intensity curve lies within the error spread of the data, the resulting concentration profile is at least as valid as results of the first approach. In so far as the constraints and assumptions eliminate physically objectionable features of the profiles and introduce new known information for the calculation, the parametric approach to the Abel inversion is better than the exact solution.

A number of trends are immediately apparent in the results of the profile-parameter calculations. First, we have the same Reynolds number independence as was noted in the earlier profile-averaged data. The jet e-folding radius $a+c$ behaves qualitatively like the ozone concentration radius. Beyond the end of the potential core, the centre-line concentration decreases in the non-reacting case; it decreases much faster in the highly reacting case. All of these trends appear in figure 5, which consists of radial ozone profiles drawn for highly reacting and for non-reacting jets at our axial stations. The profiles are plotted by assuming the profile shape (4.7). Individual values for each parameter are found by averaging the data over all runs and Reynolds numbers at the appropriate axial position and reaction state. Error bars shown represent one standard deviation in each parameter.

5. Conclusions

An optical technique has been developed to study chemical reactions in turbulent flow. This technique has been applied to the reaction occurring between ozone and nitric oxide when a turbulent jet containing ozone discharges into a dilute nitric oxide atmosphere. The measured ozone concentration can be related to the degree of mixing on the molecular scale (the 'mixedness') at all points in the jet (Shea 1976).

The experimental technique is based on the large absorption coefficient of ozone for ultraviolet radiation. A thin beam of 2537 Å light passes through the turbulent mixing zone of the axisymmetric jet which contains the ozone. During each run, the beam also traverses the mixing zone, and both beam position and beam intensity are recorded. The assumption of axial symmetry permits the calculation of the time-averaged ozone concentration $\overline{n_{O_3}}(r, z)$ from the recorded data.

At this point we can state several important conclusions about the nature of turbulence in a chemically reacting turbulent jet. First, we find a well-defined set of conditions under which the reactant profile in a chemically reacting jet becomes not only mixing limited (independent of chemical kinetics) but also independent of the concentrations of other reactants in the system, as given by (4.6a, b). The former relation identifies a regime where chemical kinetics no longer have a large impact on the profile, and the latter a regime where changes in the excess reactant concentration no longer have an impact. The two define a limit called the highly reacting jet in this work.

Second, this region of the mixing zone still containing unmixed gas from the primary jet has limits depending only on the jet geometry. The limiting reaction length and width form a uniform cylinder approximately 1·5 diameters wide and 5 diameters long.

Third, we can answer the question of when a chemical reaction is fast enough to justify critical assumptions on whether the jet is mixing limited. By considering actual measurements of a reactant profile as a function of a non-dimensional chemical kinetic rate coefficient at a fixed concentration ratio, we arrive at an operational criterion, equation (4.6a), for a mixing-limited jet. This is a considerably weaker condition than most of these mentioned in other studies (Gibson & Libby 1972; Alber & Batt 1974), which have generally compared reaction rates to Kolmogorov scales in the turbulence.

Knowledge of the actual concentration-profile shapes at each point in the jet (figure 5) provides detailed information missing in the averaged measurements. In particular, the profile shapes allow us to distinguish between unmixed gas in the potential core of the jet, where its presence has never been doubted, and unmixed gas in the mixing region of the jet. The non-reacting jet profiles of figure 5 can be related to the time-averaged mixing fraction of gas from the primary jet. The highly reacting profiles of figure 5 can be related to the probability of finding unmixed gas from the primary jet throughout the mixing zone.

The final conclusion is that increasing the Reynolds number based on nozzle diameter from 4000 to 32 000 imparts no systematic variations in excess of 10 % of the reactant concentrations. Varying the tank pressure from 1·34 to 4·0 atm and making corresponding changes in the dilution number also have no effect on the profiles. All variations must be inside the limits of experimental error, approximately a 10 % band across the average profiles of ozone concentration. The implications of the Reynolds number independence are that the presence of unmixed gas is a property of only the largest scales of the turbulence and that geometry alone controls its distribution.

This work was done at the California Institute of Technology as a Ph.D. dissertation. The author acknowledges a great deal of advice and guidance from Professor Hans W. Liepmann and Dr James E. Broadwell, who acted as his advisors. The work was supported by a contract from the U.S. Air Force.

REFERENCES

Alber, I. E. & Batt, R. G. 1974 An analysis of diffusion limited first and second order chemical reactions in a turbulent shear layer. *A.I.A.A. 7th Fluid Plasma Dyn. Conf., Palo Alto. A.I.A.A. Paper* no. 74–595.

Bradshaw, P., Ferriss, D. H. & Johnson, R. F. 1964 Turbulence in the noise-producing regions of a circular jet. *J. Fluid Mech.* **19**, 591.

Davies, P. O. A. L., Fisher, M. & Barratt, M. 1963 The characteristics of the turbulence in the mixing region of a round jet. *J. Fluid Mech.* **15**, 337.

Gibson, C. H. & Libby, P. A. 1972 On turbulent flows with fast chemical reactions. Part II. The distribution of reactants and products near a reacting surface. *Combustion Sci. Tech.* **6**, 29.

Griggs, M. 1968 Absorption coefficients on ozone in the ultraviolet and visible regions. *J. Chem. Phys.* **49**, 857.

Hawthorne, W. R., Weddell, D. S. & Hottel, H. C. 1949 Mixing and combustion in turbulent gas jets. *3rd Int. Symp. Combustion*, p. 266.

Herron, J. T. & Hine, R. E. 1973 The reaction between NO and O_3. *J. Phys. Chem. Ref. Data* **2**, 292.

Hottel, H. C. 1952 Burning in laminar and turbulent fuel jets. *4th Int. Symp. Combustion*, p. 97.

Hudson, R. D. 1971 Critical review of ultraviolet photoabsorption cross sections for molecules of astrophysical and aeronomic interest. *Nat. Stand. Ref. Data Ser., Nat. Bur. Stand.* **38**, 306.

Johnston, H. S. & Crosby, H. J. 1951 Rapid gas phase reaction between NO and O_3. *J. Chem. Phys.* **19**, 799.

Johnston, H. S. & Crosby, H. J. 1954 Kinetics of fast gas phase reaction between O_3 and NO. *J. Chem. Phys.* **22**, 689.

Jones, E. J. & Wulf, O. R. 1937 The absorptive coefficient of nitrogen pentoxide in the ultraviolet and the visible absorption spectrum of NO_3. *J. Chem. Phys.* **5**, 873.

KENT, J. H. & BILGER, R. W. 1972 Turbulent diffusion flames. *14th Int. Symp. Combustion* p. 615.

KUETHE, A. 1935 Investigations of the turbulent mixing regions formed by jets. *A.S.M.E Trans.* **2**, A-87.

MELVIN, E. H. & WULF, O. R. 1935 Ultraviolet absorption of mixtures of NO, NO_2 and H_2O *J. Chem. Phys.* **3**, 755.

SHEA, J. R. 1976 A chemical reaction in a turbulent jet. Ph.D. thesis, California Institute o Technology.

WEDDEL, D. 1941 Turbulent mixing in gas flames. Ph.D. thesis, Massachusetts Institute o Technology.

WOHL, K., GAZLEY, C. & KAPP, N. 1949 Diffusion flames. *3rd Int. Symp. Combustion*, p. 288.

YAGI, S. & SAJI, K. 1952 Problems of turbulent diffusion and flame jets. *4th Int. Symp Combustion*, p. 771.